Engineering with Computers (2022) 38 (Suppl 1):S647–S665
https://doi.org/10.1007/s00366-020-01156-y

ORIGINAL ARTICLE

Nonlocal strain gradient finite element analysis of nanobeams using two-variable trigonometric shear deformation theory

Tarek Merzouki[1] · Mohammed Sid Ahmed Houari[2] · Mohamed Haboussi[3] · Aicha Bessaim[2] · Manickam Ganapathi[4]

Received: 12 May 2020 / Accepted: 23 August 2020 / Published online: 18 September 2020
© Springer-Verlag London Ltd., part of Springer Nature 2020

Abstract

In the present paper, a new trigonometric two-variable shear deformation beam nonlocal strain gradient theory is developed and applied to investigate the combined effects of nonlocal stress and strain gradient on the bending, buckling and free vibration analysis of nanobeams. The model introduces a nonlocal stress field parameter and a length scale parameter to capture the size effect. The governing equations derived are solved employing finite element method using a 3-nodes beam element, developed for this purpose. The predictive capability of the proposed model is shown through illustrative examples for bending, buckling and free vibration of nanobeams. Comparisons with other higher-order shear deformation beam theory are also performed to validate its numerical implementation and assess its accuracy within the nonlocal context.

Keywords Nonlocal strain gradient theory · Variational formulation · Finite element method · Static analysis · Free vibration · Elastic buckling

1 Introduction

Nowadays, nanostructures such as nanorods, nanobeams and nanoplates are receiving a great attention in nanoscience and nanotechnology, due to their extraordinary mechanical, thermal, electrical, magnetic, and other properties [1–5]. Examples of applications and devices related to such nanostructures are oscillators [6], clocks [7], sensors [8–10], atomic force microscopy [11, 12], nano/micro electro-mechanical systems (NEMS/MEMS) [13, 14] and nano actuators [15, 16]. In nanostructures, the size effect is no longer negligible and becomes rather important. It is then necessary to take it account into the design of applications, such as those mentioned above. There have been many theoretical and experimental investigations for better understanding and designing the mechanical and physical behavior of such small-scaled structures [17, 18]. It is known that classical continuum mechanics is a local theory that is size-independent. So, it is not really appropriate for small-scaled structures as it does not allow to capturing the size effect in such small structures. To overcome this limitation, non-classical continuum theories are developed. Whether being of integral or gradient types, these theories utilize one or several material internal length scale parameters. Examples of such nonlocal theories are the pioneer elasticity theory of [19, 20], the strain gradient theory [21–23], the modified couple stress theory [24], and the nonlocal strain gradient theory [25]. The nonlocal elasticity theory has widely been employed to analyze the bending, vibration, buckling and wave propagation of nanostructures. Among recent works, there are [26–30], and the critical review on the topic of nanobeam and nanoplate modeling [31].

The above-mentioned studies all point out the significant influence that non-local factors can have on the static and dynamic responses of nanobeams. In particular, nonlocal elastic theory can only be used to describe material softening effect, the hardening effect reported in many experimental studies cannot be handled by such theories [32–34]. The strain gradient theory proposed by Mindlin

✉ Tarek Merzouki
tarek.merzouki@uvsq.fr

1 LISV, University of Versailles Saint-Quentin, 10-12 Avenue de l'Europe, 78140 Vélizy-Villacoublay, France

2 Laboratoire d'Etude des Structures et de Mécanique des Matériaux, University Mustapha Stambouli of Mascara, Mascara, Algeria

3 Laboratoire des Sciences des Procédés et des Matériaux (LSPM), CNRS UPR 3407, Université Paris 13, Sorbonne-Paris-Cité, 93430 Villetaneuse, France

4 School of Mechanical Engineering, VIT University, Vellore 632 014, India

[22] is a microstructure-dependent continuum theory developed to capture the hardening effect by enriching the classical continuum with additional material characteristic length scales. In this theory, the total stress is a function of additional strain gradient terms to consider microstructural deformation contributions at small scale, hence, including higher-order strain gradients [35]. Based on such nonlocal strain gradient elasticity theoretical framework, several works have been devoted to study the mechanical behavior of small scaled structures. In [24, 36–38], the linear and non-linear static, free vibration, and buckling responses of homogeneous or inhomogeneous small scaled structure are studied based on various shear deformation theories. In Li et al. [39], the flexural wave frequency response of small-scaled functionally graded Euler–Bernoulli beams is studied using a nonlocal strain gradient theory. Li et al. [40] studied the vibrational behavior of functionally graded nano/micro-scaled using a nonlocal strain gradient extension of a Timoshenko beam theory. Xu et al. [41] studied the nonlinear bending and buckling of nanobeam by a nonlocal strain gradient extension of Euler–Bernoulli beam model. Li et al. [42] examined bending, buckling and vibration of axially functionally graded beams by a nonlocal strain gradient extension of Euler–Bernoulli beam theory. Sahmani et al. [43] presented analytical solutions for nonlinear bending behavior of functionally graded porous micro/nanobeams reinforced with graphene platelets.

Allam et al. [44] analyzed the bending, buckling and vibration behaviors of viscoelastic FG curved nanobeam embedded in an elastic medium based on nonlocal strain gradient theory. Radwan et al. [45] studied the dynamic deformation of orthotropic viscoelastic graphene sheets under time harmonic thermal load. All of the previous mentioned studies were based on classical beam theory (CBT), first-order shear deformation beam theory (FSDT) and higher-order shear deformation beam theory (HSDT). The CBT is only applicable for thin beam, ignores shear deformation effects and provides reasonable results for slender beams only. However, it underestimates deflection and overestimates buckling load and frequency of moderately short or short beams [46]. The FSDT accounts for the transverse shear deformation effect and gives acceptable results for moderately short and slender beam [47], but needs a shear correction to compensate for the difference between the actual stress state and the constant stress state due to a constant shear strain assumption through the thickness [48]. In order to include shear deformation effects, several polynomial [49–51] and non polynomial [52–58] higher-order shear deformation theories (HSDTs), which are based on a non-linear variation through the thickness of the in-plane displacements, are developed. These theories provide a better prediction of response of short beam and do not require any shear correction factor and satisfy zero shear stress conditions at top and bottom surfaces of beams.

The aim of this paper is to extend the two variables trigonometric shear deformation theory of Thai [59] within a nonlocal context in order to study the bending, vibration and buckling of nanobeams. The nonlocal extension is based on the use of strain gradient constitutive relations. The most interesting features of this theory is that it accounts for a trigonometric variation of the transverse shear strains across the thickness and satisfies the zero traction boundary conditions on the top and bottom surfaces of the beam without using any shear correction factor. It should be noted that the trigonometric function was used in the first time by Levy [60] and assessed by Stein [60], and later widely used by [52] and [61]. These theories are capable of representing the section warping in the deformed configuration and the results obtained from these theories show that this theory is capable to calculate the stresses and natural frequencies more accurately than other theories. The governing equations derived are used to develop a finite element model using a 3-node beam element. Analytical solutions for bending, vibration and buckling loadings are also presented for simply supported beams. These analytical solutions are used to validate the finite element implementation of the nonlocal problem. Comparisons with existing solutions from the literature are used to assess the relevance and the accuracy of the proposed nonlocal theory in describing the mechanical behavior of nanobeam.

2 Nonlocal strain gradient theory

When dealing with nanostructures, the effect of size is important and can't be ignored in the analysis and dimensioning of the structure. In the nonlocal strain gradient elasticity, the total stress tensor is expressed as a function of the standard nonlocal stress tensor and the strain gradient stress one:

$$\sigma_{ij} = \sigma_{ij}^{(0)} - \frac{\partial \sigma_{ij}^{(1)}}{\partial x}, \tag{1}$$

where the stresses $\sigma_{ij}^{(0)}$ and $\sigma_{ij}^{(1)}$ are related to strain ε_{ij} and strain gradient $\varepsilon_{ij,x}$, respectively, and are defined as follows:

$$\sigma_{ij}^{(0)} = \int_0^L C_{ijkl}\, \alpha_0\left(x, x', e_0 a\right) \varepsilon'_{kl}\left(x'\right) \mathrm{d}x, \tag{2}$$

$$\sigma_{ij}^{(1)} = l^2 \int_0^L C_{ijkl}\, \alpha_1\left(x, x', e_1 a\right) \varepsilon'_{kl,x}\left(x'\right) \mathrm{d}x', \tag{3}$$

in which C_{ijkl} are the elastic constants, e_0a and e_1a are nonlocal parameters to consider the significance of the nonlocal stress field, l is a material length scale parameter that introduces the influence of higher-order strain gradient stress field. When the nonlocal functions $\alpha_0(x, x', e_0a)$ and $\alpha_1(x, x', e_1a)$ satisfy the developed conditions by Eringen [62–64], the constitutive relation can be stated as:

$$\left(1-(e_1a)^2\nabla^2\right)\left(1-(e_0a)^2\nabla^2\right)\sigma_{ij} = C_{ijkl}\left(\left(1-(e_1a)^2\nabla^2\right)\varepsilon_{kl} - l^2 \left(1-(e_0a)^2\nabla^2\right)\nabla^2\varepsilon_{kl}\right), \tag{4}$$

in which ∇^2 denotes the Laplacian operator. By assuming $e = e_0 = e_1$, the general constitutive equation for the size-dependent continuum can be simplified as follows:

$$\left(1-(ea)^2\nabla^2\right)\sigma_{ij} = C_{ijkl}\left(1-l^2\nabla^2\right)\varepsilon_{kl}. \tag{5}$$

Thus, the nonlocal constitutive relations for a shear deformable nanobeam can be stated as follows:

$$\begin{aligned}\sigma_{xx} - \mu\sigma_{xx}'' &= C_{11}\left(\varepsilon_{xx} - \lambda\varepsilon_{xx}''\right)\\ \sigma_{xz} - \mu\sigma_{xz}'' &= C_{66}\left(\gamma_{xz} - \lambda\gamma_{xz}''\right),\end{aligned} \tag{6}$$

where $\mu = (ea)^2$ and $\lambda = l^2$.

It is of interest that (6) can be simplified to some interested cases.

2.1 Nonlocal elasticity theory

The constitutive equation of the nonlocal elasticity theory can be easily obtained by setting $\lambda = 0$ in the nonlocal strain gradient constitutive (6) as follows:

$$\begin{aligned}\sigma_{xx} - \mu\sigma_{xx}'' &= C_{11}\varepsilon_{xx}\\ \sigma_{xz} - \mu\sigma_{xz}'' &= C_{66}\gamma_{xz},\end{aligned} \tag{7}$$

which are identical to Eringen [62–64].

2.2 Strain gradient theory

The constitutive equation of the strain gradient theory can be easily obtained by setting $\mu = 0$ in (6), that is:

$$\begin{aligned}\sigma_{xx} &= C_{11}\left(\varepsilon_{xx} - \lambda\varepsilon_{xx}''\right)\\ \sigma_{xz} &= C_{66}\left(\gamma_{xz} - \lambda\gamma_{xz}''\right),\end{aligned} \tag{8}$$

which are identical to Aifantis [65, 66].

It is shown that the general constitutive (6) can reasonably explain size-dependent phenomena and there is a good agreement between the molecular dynamics simulations and the nonlocal strain gradient theory [67, 68].

3 Governing equation for size-dependent nanobeams

To write the governing equations, we consider a straight nanobeam of length L, and a rectangular cross section $b \times h$. The variable x is taken as the cartesian coordinate along the length of the beam with $x \in [0.L]$, whereas z is assumed the coordinate along the thickness direction of the beam, and $z \in [-h/2, h/2]$. In this work, the y coordinate associated with the width direction is not considered in the formulation. Here, a wide range of slenderness ratios L/h can be studied by varying the length L and the thickness h of the beam.

3.1 Kinematics

A trigonometric shear deformation beam theory considering shear deformations is adopted in this study. The displacement field of the proposed theory is chosen based on the following assumptions: (1) the transverse displacement is partitioned into bending and shear components; (2) the axial displacement consists of extension, bending and shear components; (3) the bending component of axial displacement is similar to that given by the Euler–Bernoulli beam theory; and (4) the shear component of axial displacement gives rise to the trigonometric variation of shear strain and hence to shear stress through the thickness of the beam in such a way that shear stress vanishes on the top and bottom surfaces.

Based on the assumptions made above, the displacement field of the present theory can be obtained as:

$$\begin{aligned}u(x,z,t) &= u_0(x) - z\,w_b'(x) - f(z)\,w_s'(x)\\ w(x,z,t) &= w_b(x) + w_s(x),\end{aligned} \tag{9}$$

where u_0 is the axial displacement along the midplane of the nanoscale beam; w_b and w_s are the bending, shear components of the transverse displacement along the midplane of the beam. t is the time, derivations are denoted $(\,)' = \frac{\partial}{\partial x}$ and $\dot{(\,)} = \frac{\partial}{\partial t}$ for the time. $f(z)$ is a shape function representing the variation of the transverse shear strains and shear stresses through the thickness of the beam and is given as [69] follows:

$$f(z) = z - z\frac{\left(\pi + 2\cos\left(\frac{\pi z}{h}\right)\right)}{(\pi + 2)}. \tag{10}$$

The nonzero strains associated with the displacements field in (9) are as follows:

$$\begin{aligned}\varepsilon_x &= \varepsilon_x^0 + z\,k_x^b + f(z)\,k_x^s\\ \gamma_{xz} &= g(z)\,\gamma_{xz}^0,\end{aligned} \tag{11}$$

where

$$\varepsilon_x^0 = u_0{}', \quad k_x^b = -w_b{}'', \quad k_x^s = -w_s{}'', \quad \gamma_{xz}^0 = w_s{}' \tag{12}$$

and

$$g(z) = 1 - f'(z). \tag{13}$$

3.2 Variational statements

The governing equations of motion in terms of displacements are derived using Hamilton's Principle.

The variation of strain energy δU is expressed according to the nonlocal strain gradient theory [67]:

$$\begin{aligned}\delta U &= \int_0^L \int_{-h/2}^{h/2} \left(\sigma_{xx}^{(0)}\delta\varepsilon_{xx} + \sigma_{xz}^{(0)}\delta\gamma_{xz} + \sigma_{xx}^{(1)}\nabla\delta\varepsilon_{xx} + \sigma_{xz}^{(1)}\nabla\delta\gamma_{xz}\right)\mathrm{d}z\mathrm{d}x \\ &= \int_0^L \int_{-h/2}^{h/2} \left(\left(\sigma_{xx}^{(0)} - \nabla\sigma_{xx}^{(1)}\right)\delta\varepsilon_{xx} + \left(\sigma_{xz}^{(0)} - \nabla\sigma_{xz}^{(1)}\right)\delta\gamma_{xz}\right)\mathrm{d}z\mathrm{d}x \\ &\quad + \left[\int_0^L \int_{-h/2}^{h/2} \left(\sigma_{xx}^{(1)}\delta\varepsilon_{xx} + \sigma_{xz}^{(1)}\delta\gamma_{xz}\right)\mathrm{d}z\mathrm{d}x\right]_0^L \\ &= \int_0^L \int_{-h/2}^{h/2} \left(\sigma_{xx}\delta\gamma_{xx} + \sigma_{xz}\delta\gamma_{xz}\right)\mathrm{d}z\mathrm{d}x \\ &\quad + \left[\int_0^L \int_{-h/2}^{h/2} \left(\sigma_{xx}^{(1)}\delta\varepsilon_{xx} + \sigma_{xz}^{(1)}\delta\gamma_{xz}\right)\mathrm{d}z\mathrm{d}x\right]_0^L.\end{aligned} \tag{14}$$

$$\begin{aligned}&\delta u_0 : \ -N' = \left(-I_0\,\ddot{u}_0 + I_1\,\ddot{w}_b{}' + I_3\,\ddot{w}_s{}'\right) \\ &\delta w_b : \ -M'' - q + N_0\left(w_b{}'' + w_s{}''\right) = \left(I_1\,\ddot{u}_0 - I_2\,\ddot{w}_b{}' - I_4\,\ddot{w}_s{}' - I_0\,\ddot{w}_b - I_0\,\ddot{w}_s\right) \\ &\delta w_s : \ -\tilde{M}'' - Q' - q + N_0\left(w_b{}'' + w_s{}''\right) = \left(I_3\,\ddot{u}_0 - I_4\,\ddot{w}_b{}' - I_5\,\ddot{w}_s{}' - I_0\,\ddot{w}_b - I_0\,\ddot{w}_s\right)\end{aligned} \tag{21}$$

We define the force and the moment resultants as follow:

$$\begin{aligned}\left[N, M, \tilde{M}\right] &= \int_{-h/2}^{h/2} \left[1, z, f(z)\right]\,\sigma_{xx}\,\mathrm{d}z, \ Q = \int_{-h/2}^{h/2} \sigma_{xz}\,g(z)\,\mathrm{d}z \\ \left[N^{(1)}, M^{(1)}, \tilde{M}^{(1)}\right] &= \int_{-h/2}^{h/2} \left[1, z, f(z)\right]\,\sigma_{xx}^{(1)}\,\mathrm{d}z, \ Q^{(1)} = \int_{-h/2}^{h/2} \sigma_{xz}^{(1)}\,g(z)\,\mathrm{d}z.\end{aligned} \tag{15}$$

Thus, the virtual strain energy can be rewritten as follows:

$$\begin{aligned}\delta U = &\int_0^L \left(N\,\delta u_0{}' - M\,\delta w_b{}'' - \tilde{M}\,\delta w_s{}'' + Q\,\delta w_s{}'\right)\,\mathrm{d}x \\ &+ \left[N^{(1)}\,\delta u_0{}' - M^{(1)}\,\delta w_b{}'' - \tilde{M}^{(1)}\,\delta w_s{}'' + Q^{(1)}\,\delta w_s{}'\right]_0^L.\end{aligned} \tag{16}$$

The variation of the kinetic energy is obtained as follows:

$$\begin{aligned}\delta K = &\int_0^L \rho(\dot{u}\delta\dot{u} + \dot{w}\delta\dot{w})\,\mathrm{d}x = \int_0^L \Big(\left(-I_0\,\ddot{u}_0 + I_1\,\ddot{w}_b{}' + I_3\,\ddot{w}_s{}'\right)\delta u_0 \\ &+ \left(I_1\,\ddot{u}_0 - I_2\,\ddot{w}_b{}' - I_4\,\ddot{w}_s{}'\right)\delta w_b + \left(I_3\,\ddot{u}_0 - I_4\,\ddot{w}_b{}' - I_5\,\ddot{w}_s{}'\right)\delta w_s \\ &+ \left(-I_0\,\ddot{w}_b - I_0\,\ddot{w}_s\right)\delta w_b + \left(-I_0\,\ddot{w}_b - I_0\,\ddot{w}_s\right)\delta w_s\Big)\,\mathrm{d}x,\end{aligned} \tag{17}$$

$$\left[I_0, I_1, I_2, I_3, I_4, I_5\right] = \int_{-h/2}^{h/2} \rho\left[1, z, z^2, f(z), zf(z), f(z)^2\right]\,\mathrm{d}z. \tag{18}$$

The variation potential energy δW of external loads can be written as:

$$\delta W = -\int_0^L \left(q\,\delta w + N_0\,\left(w'\,\delta w'\right)\right)\,\mathrm{d}x, \tag{19}$$

where q is the distributed transverse load applied on the upper surface, and N_0 is the axial load acting through the mid plane.

According to Hamilton's principle, we have:

$$0 = \int_0^T (\delta U + \delta W - \delta K)\,\mathrm{d}t. \tag{20}$$

The following governing equations are derived from the variational principle (20) by introducing (16), (17), (19), and proceeding to some integrations by parts:

3.3 Nonlocal strain gradient equilibrium equations

Substituting (6) into (15), one obtains

$$\begin{aligned}&\left[(N - \mu\,N''), (M - \mu\,M''), (\tilde{M} - \mu\,\tilde{M}''), (Q - \mu\,Q'')\right] \\ &\quad = \left[N^{SG},\ M^{SG},\ \tilde{M}^{SG},\ Q^{SG}\right],\end{aligned} \tag{22}$$

with the force/moment resultants in strain gradient theory defined as follows:

$$\begin{aligned}\left[N^{SG},\ M^{SG},\ \tilde{M}^{SG}\right] &= \int_{-h/2}^{h/2} \left[1, z, f(z)\right]\,C_{11}\left(\varepsilon_{xx} - \lambda\varepsilon_{xx}{}''\right)\mathrm{d}z \\ \left[Q^{SG}\right] &= \int_{-h/2}^{h/2} \left[g(z)\right]\,C_{66}\left(\gamma_{xz} - \lambda\gamma_{xx}{}''\right)\,\mathrm{d}z.\end{aligned} \tag{23}$$

Substituting the expressions of stress and moment resultants $\left[N,\ M,\ \tilde{M},\ Q\right]$ from (22) into (21) and then simplifying the resulting equations, we obtain the following nonlocal strain gradient equations of motion as:

$$
\begin{aligned}
\delta u_0 &: -N^{SG\prime} = \left(1-\mu\frac{\mathrm{d}^2}{\mathrm{d}x^2}\right)\left(-I_0\,\ddot{u}_0 + I_1\,\ddot{w}_b{}' + I_3\,\ddot{w}_s{}'\right)\\
\delta w_b &: -M^{SG\prime\prime} = \left(1-\mu\frac{\mathrm{d}^2}{\mathrm{d}x^2}\right)\left(q - N_0\left(w_b{}'' + w_s{}''\right)\right.\\
&\qquad \left. + I_1\,\ddot{u}_0 - I_2\,\ddot{w}_b{}' - I_4\,\ddot{w}_s{}' - I_0\,\ddot{w}_b - I_0\,\ddot{w}_s\right)\\
\delta w_s &: -\tilde{M}^{SG\prime\prime} - Q' = \left(1-\mu\frac{\mathrm{d}^2}{\mathrm{d}x^2}\right)\left(q - N_0\left(w_b{}'' + w_s{}''\right)\right.\\
&\qquad \left. + I_3\,\ddot{u}_0 - I_4\,\ddot{w}_b{}' - I_5\,\ddot{w}_s{}' - I_0\,\ddot{w}_b - I_0\,\ddot{w}_s\right).
\end{aligned} \tag{24}
$$

4 Matrix formulation of the nonlocal strain gradient variational problem

From (16), (17) and (19) and introducing nonlocal strain gradient equilibrium equations (24), a finite element formulation is applied considering static, free vibration and buckling problems. After simplification, the equation is expressed in matrix form as follows:

$$
\begin{aligned}
&\int_0^L \int_{-h/2}^{h/2} \left(\{\delta\varepsilon\}^T[D]\{\varepsilon\} - \lambda\frac{d^2}{\mathrm{d}x^2}\{\delta\varepsilon\}^T[D]\{\varepsilon\}\right)\\
&= \int_0^L \left(1-\mu\frac{d^2}{\mathrm{d}x^2}\right) q\delta w \mathrm{d}x + \int_0^L \int_{-h/2}^{h/2} \left[\left(1-\mu\frac{d^2}{\mathrm{d}x^2}\right)\{\delta u\}^T\right]\rho\{\ddot{u}\}\mathrm{d}z\mathrm{d}x\\
&\quad + \int_0^L \left[\left(1-\mu\frac{d^2}{\mathrm{d}x^2}\right)\{\delta\varepsilon_u\}^T\right][k_{gg}]\{\delta\varepsilon_u\}\mathrm{d}x,
\end{aligned} \tag{25}
$$

$[D]$ denotes the elastic moduli matrix. The displacement u of (9) and the strain ε functions of (11) can be redefined as follows:

$$
\begin{aligned}
&\{u\}^T = [\mathbb{N}_u(z)]\{\mathcal{E}_u\} \quad \text{with}\\
&\{\mathcal{E}_u\}^T = \left[u_0 \;\; w_b \;\; w_s \;\; w_b{}' \;\; w_s{}'\right],
\end{aligned} \tag{26}
$$

$$
\begin{aligned}
&\{\varepsilon\}^T = [\mathbb{N}_\varepsilon(z)]\{\mathcal{E}_\varepsilon\} \quad \textit{with}\\
&\{\mathcal{E}_\varepsilon\}^T = \left[u_0{}' \;\; w_b{}' \;\; w_s{}' \;\; w_b{}'' \;\; w_s{}'',\right],
\end{aligned} \tag{27}
$$

where $\left[\mathbb{N}_u(z)\right]$ and $\left[\mathbb{N}_\varepsilon(z)\right]$ depend only on the normal coordinate z, and are defined as follows:

$$
[\mathbb{N}_u(z)] = \begin{bmatrix} 1 & 0 & 0 & -z & f(z) \\ 0 & 1 & 1 & 0 & 0, \end{bmatrix} \tag{28}
$$

$$
[\mathbb{N}_\varepsilon(z)] = \begin{bmatrix} 1 & 0 & 0 & -z & f(z) \\ 0 & 0 & 1+f(z)' & 0 & 0. \end{bmatrix} \tag{29}
$$

Equation (25) can be expanded as follows:

$$
\begin{aligned}
&\int_0^L \left(\{\delta\mathcal{E}_\varepsilon\}^T[k_{\varepsilon\varepsilon}]\{\mathcal{E}_\varepsilon\} - \lambda\frac{d^2}{\mathrm{d}x^2}\{\delta\mathcal{E}_\varepsilon\}^T[k_{\varepsilon\varepsilon}]\{\mathcal{E}_\varepsilon\}\right)\mathrm{d}x\\
&= \int_0^L \left(1-\mu\frac{d^2}{\mathrm{d}x^2}\right) q\delta w\,\mathrm{d}x\\
&\quad + \int_0^L \left(1-\mu\frac{d^2}{\mathrm{d}x^2}\right)\{\delta\mathcal{E}_u\}^T[m_{uu}]\{\ddot{\mathcal{E}}_u\}\,\mathrm{d}x\\
&\quad + \int_0^L \left(1-\mu\frac{d^2}{\mathrm{d}x^2}\right)\{\delta\mathcal{E}_u\}^T[k_{gg}]\{\mathcal{E}_u\}\,\mathrm{d}x,
\end{aligned} \tag{30}
$$

where

$$
[k_{\varepsilon\varepsilon}] = \int_{-h/2}^{h/2} [\mathbb{N}_\varepsilon(z)]^T[D][\mathbb{F}_\varepsilon(z)]\mathrm{d}z, \tag{31}
$$

$$
[m_{uu}] = \int_{-h/2}^{h/2} \rho[\mathbb{N}_u(z)]^T[\mathbb{N}_u(z)]\mathrm{d}z. \tag{32}
$$

$[k_{\varepsilon\varepsilon}]$ is the stiffness matrix, $[m_{uu}]$ is the masse matrix. $[k_{gg}]$ is the geometric stiffness matrix of 5×5 dimensions, is symmetric and the non zero terms are as follows:

$$
k_{gg}(4,4)=1,\;\; k_{gg}(4,5)=1,\;\; k_{gg}(5,4)=1,\;\; k_{gg}(5,5)=1. \tag{33}
$$

The weak forme is then applied considering static problems, and the equation is simplified after integration by parts on RHS:

$$
\begin{aligned}
&\int_0^L \left(\{\delta\mathcal{E}_\varepsilon\}^T[k_{\varepsilon\varepsilon}]\{\mathcal{E}_\varepsilon\} - \lambda\{\delta\mathcal{E}_\varepsilon{}''\}^T[k_{\varepsilon\varepsilon}]\{\mathcal{E}_\varepsilon{}''\}\right)\mathrm{d}x\\
&= \int_0^L \left(\delta w - \mu w''\right) q\delta\,\mathrm{d}x.
\end{aligned} \tag{34}
$$

For free vibration analysis, after performing integration by parts, a weak form is derived for the following dynamic equation:

$$
\begin{aligned}
&\int_0^L \left(\{\delta\mathcal{E}_\varepsilon\}^T[k_{\varepsilon\varepsilon}]\{\mathcal{E}_\varepsilon\} - \lambda\{\delta\mathcal{E}_\varepsilon{}''\}^T[k_{\varepsilon\varepsilon}]\{\mathcal{E}_\varepsilon{}''\}\right)\mathrm{d}x\\
&= \int_0^L \left(\{\delta\mathcal{E}_u\}^T[m_{uu}]\{\ddot{\mathcal{E}}_u\} + \mu\{\delta\mathcal{E}_u{}''\}^T[m_{uu}]\{\ddot{\mathcal{E}}_u{}''\}\right).
\end{aligned} \tag{35}
$$

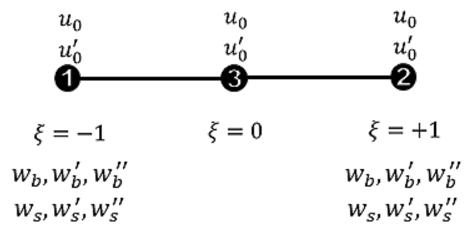

Fig. 1 Beam element with the degrees of freedom per node

with $[N_u]$ and $[N_w]$ being the Hermite interpolation functions, q_{u_0} and q_w are the nodal degrees of freedom (dof) vectors of each elementary element (Fig. 1) while subscripts 1–2–3 are the node numbers ($\xi = -1, 0, +1$) (Fig. 1).

Let us consider the following vector q_e of total nodal dof for a generic elementary domain Ω_e:

$$\{q_e\}^T = \left[u_0^{(1)}\ u_0'^{(1)}\ w_b^{(1)}\ w_b'^{(1)}\ w_b''^{(1)}\ w_s^{(1)}\ w_s'^{(1)}\ w_s''^{(1)}\ u_0^{(3)}\ u_0'^{(3)}\ u_0^{(2)}\ u_0'^{(2)}\ w_b^{(2)}\ w_b'^{(2)}\ w_b''^{(2)}\ w_s^{(2)}\ w_s'^{(2)}\ w_s''^{(2)}\right]. \tag{40}$$

Considering buckling problem subjected to axial force N_0 applied in the mid plane, the weak form is given after integration by parts on RHS as follows:

$$\int_0^L \left(\{\delta\mathcal{E}_\varepsilon\}^T[k_{\varepsilon\varepsilon}]\{\mathcal{E}_\varepsilon\} - \lambda\{\delta\mathcal{E}_\varepsilon''\}^T[k_{\varepsilon\varepsilon}]\{\mathcal{E}_\varepsilon''\}\right)\mathrm{d}x = \int_0^L \left(\{\delta\mathcal{E}_u\}^T[k_{gg}]\{\ddot{\mathcal{E}}_u\} + \mu\{\delta\mathcal{E}_u''\}^T[k_{gg}]\{\ddot{\mathcal{E}}_u''\}\right). \tag{36}$$

The above equations are used for FE modelenig, and this will be described in the next section.

5 Finite element approximations

To develop the finite element model, the beam is discretized into a set of elements of length l_e. The beam element given in Fig. 1 is defined by three nodes along the element local x-axis. The nodal coordinates x is approximated based on the reference length with respect to the reduced coordinate ξ by the following:

$$x(\xi) = \frac{1+\xi}{2}\, l_e. \tag{37}$$

The generalized displacements and strain are given in (9) and (11) and have to be approximated by finite element method. In the present work, the Hermite interpolation is employed to satisfy C^1 and C^2 continuity requirement for the axial and transversal displacements, respectively. The displacements $u_0(\xi)$ and $w_i(\xi)$ are defined as follows:

$$\begin{aligned}\{u_0\} &= [N_u]\{q_{u_0}\}\\ \{w_i\} &= [N_w]\ \{q_{w_i}\}|_{i=b,s},\end{aligned} \tag{38}$$

where

$$\begin{aligned}\{q_{u_0}\}^T &= [u_0^{(1)}\ u_0'^{(1)}\ u_0^{(3)}\ u_0'^{(3)}\ u_0^{(2)}\ u_0'^{(2)}]\\ \{q_{w_i}\}^T &= [w_i^{(1)}\ w_i'^{(1)}\ w_i''^{(1)}\ w_i^{(2)}\ w_i'^{(2)}\ w_i''^{(2)}]|_{i=b,s},\end{aligned} \tag{39}$$

From (26) and (27), the vectors $\{\varepsilon_u\}$ and $\{\varepsilon_\varepsilon\}$ are expressed from the dof vector $\{q_e\}$ using (38) and (39):

$$\begin{aligned}\{\varepsilon_u\} &= [B_u]\{q_e\}\\ \{\varepsilon_\varepsilon\} &= [B_\varepsilon]\{q_e\}\\ \{w_i''\} &= [N_w'']^T\{q_{w_i}\}, \quad i = b, s\\ \{\varepsilon_u'\} &= [B_u']\{q_e\}\\ \{\varepsilon_\varepsilon'\} &= [B_\varepsilon']\{q_e\},\end{aligned} \tag{41}$$

where $[B_u]$ and $[B_\varepsilon]$ are 5×18 and 2×18 matrices, respectively, containing the shape function N_u, N_w and their derivative terms.

The final expressions of the system could be written as follows:

- Static analysis: a transversal load q is applied on the top surface of the beam, and we have the following system to solve:

$$[K]\{q\} = \{F\}. \tag{42}$$

- Free vibration analysis:

$$\left([K] - \omega^2[M]\right)\{q\} = \{0\}. \tag{43}$$

- Buckling analysis: a constant axial force is acting through the mid-line and the deduce system is given by

$$\left([K] - N_0[K_g]\right)\{q\} = \{0\}, \tag{44}$$

where $\{q\}$ is the global dof vector of the beam.

$[K]$, $[M]$ and $[K_g]$, are the stiffness, mass and geometric stiffness matrices, respectively, and $\{F\}$ is the load vector. They are obtained by assembling the individual element contributions using the elementary matrices given as follows:

Where $\{q\}$ is the global dof vector of the beam. $[K]$ is global the stiffness matrix, $[M]$ is the mass matrix, $[K_g]$ is the geometric stiffness matrix and $\{F\}$ is the load vector. They are obtained by assembling the individual element contributions using the elementary matrices given as follows:

$$
\begin{aligned}
[K_e] &= \int_0^l \left([B_\varepsilon]^T[k_{\varepsilon\varepsilon}][B_\varepsilon] + \lambda[B_\varepsilon{}']^T[k_{\varepsilon\varepsilon}][B_\varepsilon{}']\right) \mathrm{d}x \\
[M_e] &= \int_0^l \left([B_u]^T[m_{uu}][B_u] + \mu[B_u{}']^T[m_{uu}][B_u{}']\right) \mathrm{d}x \\
[K_{ge}] &= \int_0^l \left([B_u]^T[k_{gg}][B_u] + \mu[B_u{}']^T[k_{gg}][B_u{}']\right) \mathrm{d}x \\
\{F_e\} &= q\int_0^l \left(\{N_w\}^T - \mu\{N_w''\}^T\right) \mathrm{d}x.
\end{aligned}
\tag{45}
$$

6 Results and discussion

The first results are presented to test the robustness of the developed finite element model by considering problems for which analytical solutions are available. The study is carried out by varying parameters such as slenderness ratio $S = L/h$, nonlocal and strain gradient parameters ($\mu = ea^2, \lambda = l^2$). The results are presented to show the size dependency in the nonlocal response of the nanobeams.

The considered problem is presented as a straight nanobeams with fixed thickness $h = 10$ nm, and the length L (nm) is considered to be a variable. Different values of the slenderness ratio are considered allowing to study thick to thin beams $S = \{5, 10, 20, 50\}$. The values for nonlocal parameter $\mu\,(\mathrm{nm}^2) = (ea)^2$ for the detailedd analysis are assumed to belong to $\{0, 1, 2, 3, 4\}$. The strain gradient parameter $\lambda\,(\mathrm{nm}^2) = l^2$ is considered to belong to $\{0, 1, 2, 3, 4\}$. Different Boundary conditions are considered, simply supported beam, clamped-simply supported, clamped–clamped, cantilever beam. The considered material is an isotropic with Young modulus E and Poisson's ratio ν. In the present paper, the following dimensionless quantities are introduced:

$$
\begin{aligned}
\bar{w} &= w\frac{100E}{qhS^4} \\
\bar{\omega} &= \omega L^2\sqrt{\frac{m}{EI}},\ m = \rho h,\ I = \frac{h^3}{12} \\
\bar{N} &= N_0\frac{L^2}{EI}
\end{aligned}
$$

6.1 Assessment of the present formulation

To verify the reliability of the present formulation, an assessment of the present formulation is carried out on a simply supported nanobeams subjected to uniform load. Before proceeding to the analysis, a convergence study is considered by varying the number of elements for both local and nonlocal nanobeams. The results are presented in Tables 1, 2 and 3 along with those of analytical solutions obtained using Navier approach. The tables present the dimensionless maximum deflection, dimensionless buckling loads and dimensionless fundamental frequency, respectively, for different values of slenderness ratio (L/h), nonlocal parameter (ea) and strain gradient parameter (l). It is seen from these tables that four elements' idealization is sufficient in obtaining converged results.

It can be seen that the nonlocal parameter and the strain gradient parameter have significant effects on the response of the nanobeam. With increasing in nonlocal parameter value, the dimensionless deflection value increases and the dimensionless critical buckling load and the frequency value decrease. Nonlocal parameter μ and strain gradient parameter l have the opposite effect. The results are compared to the analytical ones obtained using Navier approach and with those available in the literature [17, 18]. It is seen that from tables, the results obtained using the present formulation are found to be in good agreement with the analytical ones and with those in the literature.

Figures 2, 3 and 4 illustrate the influence of slenderness ratio of the simply supported nanobeam for different values of nonlocal and strain gradient parameters. It is clearly seen that when the nonlocal effect dominates $ea > l$, the dimensionless deflection is larger than those obtained by classical continuum theory $l = ea$, and the nanobeam is softened and becomes easy to deform. Also, the dimensionless buckling loads and the dimensionless fundamental frequency are lower than those of classical theory. However, when the strain gradient effect dominates $l > ea$, the deflection is lower than those of classical continuum theory $l = ea$, and the nanobeam is hardened and becomes difficult to deform. This is opposite to the case of buckling and vibration response. In addition, with the increasing slenderness ratio, the dimensionless deflection decreases when $ea > l$ and increases when $l > ea$, which is also counter to the situation of buckling and vibration response. Also, it can be seen that the differences between results predicted by classical theory and nonlocal strain gradient are significant for lower values of slenderness ratio but they are diminishing as the increase of slenderness ratio. Similar conclusions have also been observed about dynamic response based on the nonlocal strain gradient theory [17, 18, 40, 70].

6.2 Bending, vibration and buckling analysis of nanobeams

The second result is a nanobeam with one end fixed and the other simply supported. Tables 4, 5 and 6 depict the dimensionless maximum deflection, dimensionless buckling loads and dimensionless fundamental frequency for different values of nonlocal parameter (ea), strain gradient parameter (l) and slenderness ratio (L/h). From the tables, the deflection decreases with increase in nonlocal parameter value, the dimensionless critical buckling load and the dimensionless frequency decreases. The strain gradient parameter l has a

Table 1 Comparison of dimensionless maximum deflections of simply supported nanobeam

ea (nm)	Beam theory	$L/h = 10$			$L/h = 20$			$L/h = 50$		
		$l = 0$ nm	$l = 1$ nm	$l = 2$ nm	$l = 0$ nm	$l = 1$ nm	$l = 2$ nm	$l = 0$ nm	$l = 1$ nm	$l = 2$ nm
0	**Present (FEM)**									
	No of elements									
	2	1.3345	1.2168	0.9598	1.3102	1.2794	1.1945	1.3034	1.2984	1.2836
	4	1.3344	1.2167	0.9597	1.3102	1.2794	1.1944	1.3034	1.2984	1.2836
	8	1.3344	1.2167	0.9597	1.3102	1.2794	1.1944	1.3034	1.2984	1.2836
	16	1.3344	1.2167	0.9597	1.3102	1.2794	1.1944	1.3034	1.2984	1.2836
	32	1.3344	1.2167	0.9597	1.3102	1.2794	1.1944	1.3034	1.2984	1.2836
	Present (Navier)	1.3344	1.2167	0.9597	1.3102	1.2794	1.1944	1.3034	1.2984	1.2836
	EBT [18]	1.3021	1.1870	0.9360	1.3021	1.2715	1.1870	1.3021	1.2971	1.2823
	TBT [18]	1.3346	1.2169	0.9598	1.3102	1.2794	1.1944	1.3034	1.2984	1.2836
	TSDBT [18]	1.3346	1.2169	0.9598	1.3102	1.2794	1.1944	1.3034	1.2984	1.2836
	SSDBT [18]	1.3345	1.2168	0.9597	1.3102	1.2794	1.1944	1.3034	1.2984	1.2836
	HSDBT [18]	1.3346	1.2169	0.9598	1.3102	1.2794	1.1944	1.3034	1.2984	1.2836
	ESDBT [18]	1.3344	1.2167	0.9596	1.3102	1.2794	1.1944	1.3034	1.2984	1.2836
	ASDBT [18]	1.3344	1.2167	0.9596	1.3102	1.2794	1.1944	1.3034	1.2984	1.2836
1	**Present (FEM)**									
	No of elements									
	2	1.4623	1.3344	1.0534	1.3416	1.3102	1.2234	1.3084	1.3034	1.2886
	4	1.4619	1.3344	1.0533	1.3416	1.3102	1.2233	1.3084	1.3034	1.2886
	8	1.4620	1.3344	1.0533	1.3416	1.3102	1.2233	1.3084	1.3034	1.2886
	16	1.4620	1.3344	1.0533	1.3416	1.3102	1.2233	1.3084	1.3034	1.2886
	32	1.4620	1.3344	1.0533	1.3416	1.3102	1.2233	1.3084	1.3034	1.2886
	Present (Navier)	1.4620	1.3344	1.0533	1.3416	1.3102	1.2234	1.3084	1.3034	1.2886
	EBT [18]	1.4271	1.3021	1.0275	1.3333	1.3021	1.2157	1.3071	1.3021	1.2873
	TBT [18]	1.4622	1.3346	1.0535	1.3416	1.3102	1.2234	1.3084	1.3034	1.2886
	TSDBT [18]	1.4622	1.3346	1.0535	1.3416	1.3102	1.2234	1.3084	1.3034	1.2886
	SSDBT [18]	1.4621	1.3345	1.0534	1.3416	1.3102	1.2234	1.3084	1.3034	1.2886
	HSDBT [18]	1.4622	1.3346	1.0535	1.3416	1.3102	1.2234	1.3084	1.3034	1.2886
	ESDBT [18]	1.4620	1.3344	1.0533	1.3416	1.3102	1.2233	1.3084	1.3034	1.2886
	ASDBT [18]	1.4620	1.3344	1.0533	1.3416	1.3102	1.2233	1.3084	1.3034	1.2886
1	**Present (FEM)**									
	No of elements									
	2	1.8460	1.6872	1.3344	1.4359	1.4024	1.3102	1.3234	1.3183	1.3034
	4	1.8445	1.6875	1.3344	1.4358	1.4025	1.3102	1.3234	1.3183	1.3034
	8	1.8447	1.6875	1.3344	1.4358	1.4025	1.3102	1.3234	1.3183	1.3034
	16	1.8447	1.6875	1.3344	1.4358	1.4025	1.3102	1.3234	1.3183	1.3034
	32	1.8447	1.6875	1.3344	1.4358	1.4025	1.3102	1.3234	1.3183	1.3034
	Present (Navier)	1.8447	1.6875	1.3344	1.4359	1.4026	1.3102	1.3234	1.3184	1.3034
	EBT [18]	1.8021	1.6475	1.3021	1.4271	1.3940	1.3021	1.3221	1.3170	1.3021
	TBT [18]	1.8450	1.6877	1.3346	1.4359	1.4026	1.3102	1.3234	1.3184	1.3034
	TSDBT [18]	1.8450	1.6877	1.3346	1.4359	1.4026	1.3102	1.3234	1.3184	1.3034
	SSDBT [18]	1.8449	1.6876	1.3345	1.4358	1.4026	1.3102	1.3234	1.3184	1.3034
	HSDBT [18]	1.8450	1.6877	1.3346	1.4359	1.4026	1.3102	1.3234	1.3184	1.3034
	ESDBT [18]	1.8447	1.6874	1.3344	1.4358	1.4025	1.3102	1.3234	1.3183	1.3034
	ASDBT [18]	1.8447	1.6874	1.3344	1.4358	1.4025	1.3102	1.3234	1.3183	1.3034

Table 2 Comparison of dimensionless buckling loads of simply supported nanobeam

ea (nm)	Beam theory	$L/h = 10$			$L/h = 20$			$L/h = 50$		
		$l = 0$ nm	$l = 1$ nm	$l = 2$ nm	$l = 0$ nm	$l = 1$ nm	$l = 2$ nm	$l = 0$ nm	$l = 1$ nm	$l = 2$ nm
0	**Present (FEM)**									
	No of elements									
	2	9.6241	10.5740	13.4240	9.8070	10.0491	10.7751	9.8596	9.8985	10.0153
	4	9.6240	10.5739	13.4235	9.8070	10.0490	10.7749	9.8595	9.8985	10.0152
	8	9.6240	10.5739	13.4234	9.8070	10.0490	10.7749	9.8595	9.8985	10.0152
	16	9.6240	10.5739	13.4234	9.8070	10.0490	10.7749	9.8595	9.8985	10.0152
	32	9.6240	10.5739	13.4234	9.8070	10.0490	10.7749	9.8595	9.8985	10.0152
	Present (Navier)	9.6251	10.5751	13.4250	9.8073	10.0493	10.7753	9.8596	9.8985	10.0152
	EBT [18]	9.8696	10.8437	13.7660	9.8696	10.1131	10.8437	9.8696	9.9086	10.0255
	TBT [18]	9.6227	10.5724	13.4216	9.8067	10.0487	10.7746	9.8595	9.8984	10.0152
	TSDBT [18]	9.6228	10.5725	13.4217	9.8067	10.0487	10.7746	9.8595	9.8984	10.0152
	SSDBT [18]	9.6231	10.5729	13.4222	9.8068	10.0488	10.7747	9.8595	9.8984	10.0152
	HSDBT [18]	9.6228	10.5725	13.4217	9.8067	10.0487	10.7746	9.8595	9.8984	10.0152
	ESDBT [18]	9.6242	10.5741	13.4237	9.8071	10.0491	10.7750	9.8595	9.8985	10.0152
	ASDBT [18]	9.6242	10.5741	13.4237	9.8071	10.0491	10.7750	9.8595	9.8985	10.0152
1	**Present (FEM)**									
	No of elements									
	2	8.7595	9.6242	12.2181	9.5709	9.8071	10.5156	9.8208	9.8596	9.9759
	4	8.7595	9.6240	12.2176	9.5709	9.8070	10.5155	9.8208	9.8595	9.9758
	8	8.7595	9.6240	12.2176	9.5709	9.8070	10.5155	9.8208	9.8595	9.9758
	16	8.7595	9.6240	12.2176	9.5709	9.8070	10.5155	9.8208	9.8595	9.9758
	32	8.7595	9.6240	12.2176	9.5709	9.8070	10.5155	9.8208	9.8595	9.9758
	Present (Navier)	8.7605	9.6251	12.2190	9.5712	9.8073	10.5158	9.8208	9.8596	9.9758
	EBT [18]	8.9830	9.8696	12.5294	9.6320	9.8696	10.5826	9.8308	9.8696	9.9860
	TBT [18]	8.7583	9.6227	12.2159	9.5706	9.8067	10.5151	9.8207	9.8595	9.9758
	TSDBT [18]	8.7583	9.6228	12.2160	9.5706	9.8067	10.5151	9.8207	9.8595	9.9758
	SSDBT [18]	8.7587	9.6231	12.2165	9.5706	9.8068	10.5152	9.8207	9.8595	9.9758
	HSDBT [18]	8.7583	9.6228	12.2160	9.5706	9.8067	10.5151	9.8207	9.8595	9.9758
	ESDBT [18]	8.7597	9.6242	12.2179	9.5709	9.8071	10.5155	9.8208	9.8595	9.9759
	ASDBT [18]	8.7597	9.6242	12.2179	9.5709	9.8071	10.5155	9.8208	9.8595	9.9759
2	**Present (FEM)**									
	No of elements									
	2	6.9000	7.5811	9.6244	8.9261	9.1464	9.8072	9.7063	9.7446	9.8596
	4	6.9000	7.5810	9.6240	8.9261	9.1463	9.8070	9.7063	9.7446	9.8595
	8	6.9000	7.5810	9.6240	8.9261	9.1463	9.8070	9.7063	9.7446	9.8595
	16	6.9000	7.5810	9.6240	8.9261	9.1463	9.8070	9.7063	9.7446	9.8595
	32	6.9000	7.5810	9.6240	8.9261	9.1463	9.8070	9.7063	9.7446	9.8595
	Present (Navier)	6.9008	7.5819	9.6251	8.9263	9.1467	9.8073	9.7063	9.7446	9.8596
	EBT [18]	7.0761	7.7745	9.8696	8.9830	9.2047	9.8696	9.7162	9.7545	9.8696
	TBT [18]	6.8990	7.5800	9.6227	8.9258	9.1460	9.8067	9.7062	9.7445	9.8595
	TSDBT [18]	6.8991	7.5800	9.6228	8.9258	9.1460	9.8067	9.7062	9.7445	9.8595
	SSDBT [18]	6.8994	7.5803	9.6231	8.9258	9.1461	9.8068	9.7062	9.7445	9.8595
	HSDBT [18]	6.8991	7.5800	9.6228	8.9258	9.1460	9.8067	9.7062	9.7445	9.8595
	ESDBT [18]	6.9002	7.5812	9.6242	8.9261	9.1463	9.8071	9.7063	9.7446	9.8595
	ASDBT [18]	6.9002	7.5812	9.6242	8.9261	9.1463	9.8071	9.7063	9.7446	9.8595

Table 3 Comparison of dimensionless fundamental frequency of simply supported nanobeam

ea (nm)	Beam theory	$L/h = 10$			$L/h = 50$		
		$l = 0$ nm	$l = 0.5$ nm	$l = 1$ nm	$l = 0$ nm	$l = 0.5$ nm	$l = 1$ nm
0	**Present (FEM)**						
	No of elements						
	2	9.7082	9.8272	10.1760	9.8630	9.8678	9.8824
	4	9.7082	9.8272	10.1760	9.8630	9.8678	9.8824
	8	9.7082	9.8272	10.1760	9.8630	9.8678	9.8824
	16	9.7082	9.8272	10.1760	9.8630	9.8678	9.8824
	32	9.7082	9.8272	10.1760	9.8630	9.8678	9.8824
	Present (Navier)	9.7082	9.8272	10.1760	9.8630	9.8678	9.8824
	EBT [17]	9.8293	9.9498	10.3029	9.8680	9.8728	9.8874
	TBT [17]	9.7075	9.8265	10.1753	9.8629	9.8678	9.8824
	SBT [17]	9.7077	9.8267	10.1755	9.8629	9.8678	9.8824
1	**Present (FEM)**						
	No of elements						
	2	9.2619	9.3754	9.7082	9.8435	9.8484	9.8630
	4	9.2618	9.3754	9.7082	9.8435	9.8484	9.8630
	8	9.2618	9.3754	9.7082	9.8435	9.8484	9.8630
	16	9.2618	9.3754	9.7082	9.8435	9.8484	9.8630
	32	9.2618	9.3754	9.7082	9.8435	9.8484	9.8630
	Present (Navier)	9.2618	9.3754	9.7082	9.8435	9.8484	9.8630
	EBT [17]	9.3774	9.4924	9.8293	9.8486	9.8534	9.8680
	TBT [17]	9.2612	9.3748	9.7075	9.8435	9.8484	9.8629
	SBT [17]	9.2614	9.3750	9.7077	9.8435	9.8484	9.8629
0	**Present (FEM)**						
	No of elements						
	2	8.2202	8.3210	8.6164	9.7860	9.7908	9.8053
	4	8.2202	8.3210	8.6163	9.7860	9.7908	9.8053
	8	8.2202	8.3210	8.6163	9.7860	9.7908	9.8053
	16	8.2202	8.3210	8.6163	9.7860	9.7908	9.8053
	32	8.2202	8.3210	8.6163	9.7860	9.7908	9.8053
	Present (Navier)	8.2202	8.3210	8.6163	9.7860	9.7908	9.8053
	EBT [17]	8.3228	8.4248	8.7238	9.7910	9.7958	9.8103
	TBT [17]	8.2196	8.3204	8.6157	9.7860	9.7908	9.8053
	SBT [17]	8.2198	8.3206	8.6159	9.7860	9.7908	9.8053

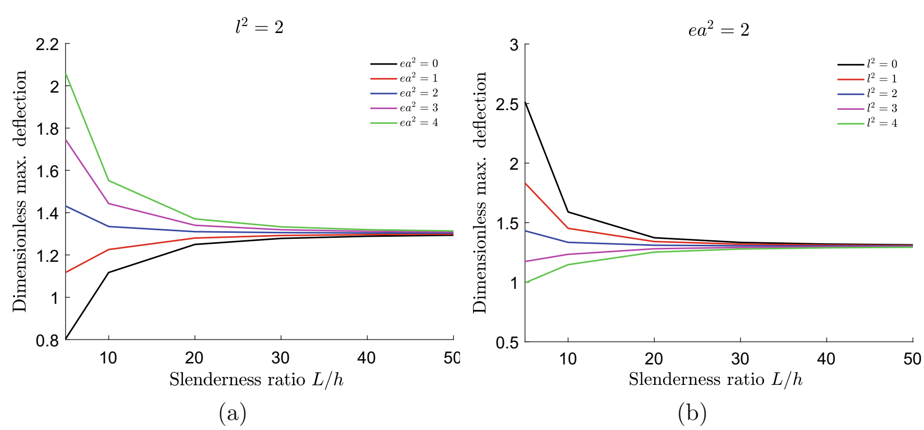

Fig. 2 Simply supported nanobeam: effect of slenderness ratio (L/h) on the deflections, **a** for different values of nonlocal parameter with $l^2 = 2$, **b** for different values of strain gradient parameter with $ea^2 = 2$

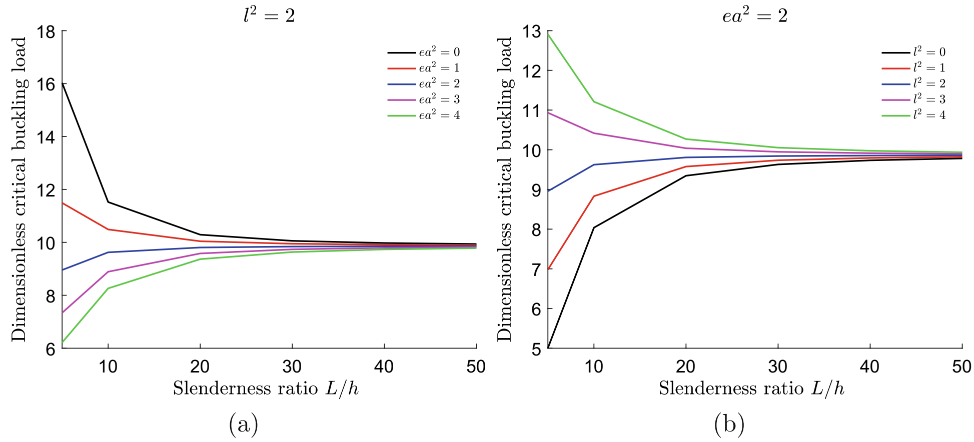

Fig. 3 Simply supported nanobeam: effect of slenderness ratio (*L*/*h*) on the buckling, **a** for different values of nonlocal parameter with $l^2 = 2$, **b** for different values of strain gradient parameter with $ea^2 = 2$

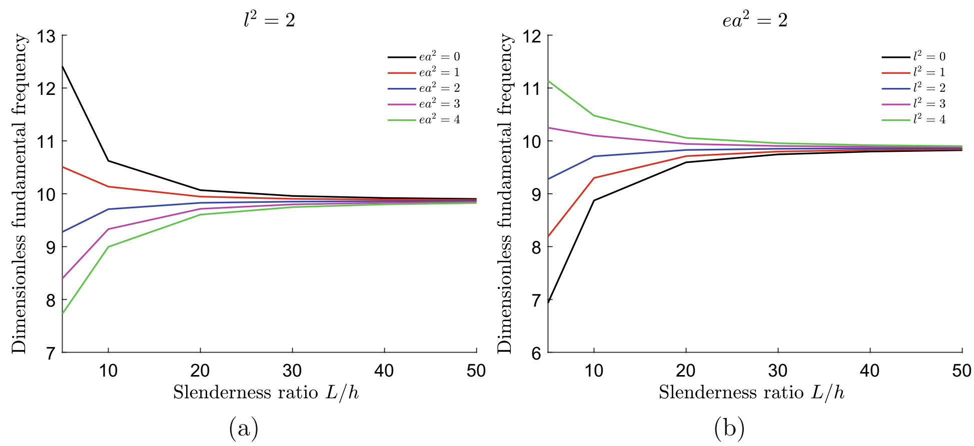

Fig. 4 Simply supported nanobeam: effect of slenderness ratio (*L*/*h*) on the free vibration, **a** for different values of nonlocal parameter with $l^2 = 2$, **b** for different values of strain gradient parameter with $ea^2 = 2$

Table 4 Clamped-simply nanobeam: dimensionless maximum deflections

ea (nm)	$L/h = 10$			$L/h = 20$			$L/h = 50$		
	$l = 0$ nm	$l = 1$ nm	$l = 2$ nm	$l = 0$ nm	$l = 1$ nm	$l = 2$ nm	$l = 0$ nm	$l = 1$ nm	$l = 2$ nm
0	0.5478	0.3195	0.1706	0.5240	0.4098	0.3018	0.5174	0.4747	0.4272
1	0.5801	0.3411	0.1831	0.5319	0.4164	0.3070	0.5186	0.4759	0.4283
2	0.6771	0.4060	0.2203	0.5554	0.4362	0.3226	0.5223	0.4794	0.4316

tendency to decrease the dimensionless deflection and also to increase the buckling load and the frequency.

The influence of slenderness ratio, the nonlocal parameter and strain gradient parameter is brought in Figs. 5, 6 and 7. According to the figures, it can be observed that the effects of the nonlocal and strain gradient parameters are qualitatively similar to that of simply supported nanobeam. However, with the increasing of slenderness ratio, the dimensionless deflection increases when $l > ea$ or when $l < ea$. Also, contrary to the simply supported case, the differences between the dimensionless deflection predicted by classical theory and nonlocal strain gradient are weak for lower values of slenderness ratio, and they are diminishing as the increase of slenderness ratio.

The third analysis is performed assuming clamped–clamped straight nanobeams under a uniform load for the bending analysis. The dimensionless maximum deflection, dimensionless buckling loads and dimensionless fundamental frequency are highlighted in Tables 7, 8 and 9 assuming different nonlocal parameter and strain gradient parameter. It can be noted that the dimensionless maximum deflection are not affected by the nonlocal parameter, and the dimensionless maximum deflection decreases with the increase of strain gradient parameter λ. The results are qualitatively similar to that of clamped-simply supported beam with no effect of nonlocal parameter. The influence of slenderness ratio, the nonlocal parameter and strain gradient parameter are brought in Figs. 8, 9 and 10.

Table 5 Clamped-simply nanobeam: dimensionless buckling loads

L/*h*	*ea* (nm)	First buckling load			Second buckling load			Third buckling load		
		$l = 0$ nm	$l = 1$ nm	$l = 2$ nm	$l = 0$ nm	$l = 1$ nm	$l = 2$ nm	$l = 0$ nm	$l = 1$ nm	$l = 2$ nm
5	0	2.4155	3.8287	5.8249	18.1308	39.3600	87.7649	37.9108	136.5981	404.3530
	1	2.1977	3.4132	5.0733	9.5836	18.3065	39.9924	10.9021	52.7773	180.7486
	2	1.7298	2.5469	3.5993	3.4750	11.7276	15.4692	3.9696	15.4980	53.2982
10	0	2.4616	3.0773	3.9339	21.0819	29.9254	46.5778	53.4035	94.7720	195.4781
	1	2.4021	2.9959	3.8182	17.2383	23.9431	36.2702	32.9784	55.5343	112.3988
	2	2.2397	2.7748	3.5059	11.1435	14.7124	21.3196	15.3574	23.9315	49.8174
20	0	2.4734	2.7442	3.0953	21.9796	25.4217	31.3975	59.5513	74.4738	106.6443
	1	2.4582	2.7265	3.0744	20.8192	24.0194	29.5614	51.5669	64.0462	90.7834
	2	2.4136	2.6749	3.0134	17.9724	20.5975	25.1076	36.7749	44.9262	62.2120
50	0	2.4768	2.5709	2.6863	22.2451	23.2645	24.8194	61.5403	65.3204	72.4764
	1	2.4743	2.5683	2.6835	22.0485	23.0556	24.5922	60.0525	63.7166	70.6604
	2	2.4670	2.5606	2.6753	21.4789	22.4507	23.9344	55.9917	59.3429	65.7140

Table 6 Clamped-simply nanobeam: dimensionless fundamental frequencies

L/*h*	*ea* (nm)	First mode			Second mode			Third mode		
		$l = 0$ nm	$l = 1$ nm	$l = 2$ nm	$l = 0$ nm	$l = 1$ nm	$l = 2$ nm	$l = 0$ nm	$l = 1$ nm	$l = 2$ nm
5	0	3.4254	5.0103	6.7106	18.5342	29.4441	43.0438	27.2417	84.0706	43.0438
	1	3.1515	4.4874	5.8972	12.7079	18.7541	26.9064	23.6772	42.9708	71.6460
10	0	3.5028	4.2674	5.1639	21.0100	26.7584	34.4589	55.3320	76.9570	108.9553
	1	3.4244	4.1545	5.0079	18.3362	22.8261	28.7976	42.2444	56.7013	78.8647
	2	3.2153	3.8596	4.6080	14.0481	17.0436	21.1093	28.6743	37.9554	53.0279
20	0	3.5233	3.8819	4.2973	21.8264	24.4156	27.9957	60.0283	69.4160	84.5772
	1	3.5030	3.8574	4.2678	20.9969	23.4030	26.7284	55.0325	63.1483	76.2705
	2	3.4438	3.7863	4.1825	18.9742	20.9782	23.7531	45.3876	51.4739	61.4571
50	0	3.5292	3.6591	3.8106	22.0758	22.9504	24.0898	61.6279	64.4705	68.8419
	1	3.5259	3.6556	3.8067	21.9337	22.7974	23.9228	60.6962	63.4614	67.7211
	2	3.5161	3.6450	3.7953	21.5227	22.3554	23.4414	58.1370	60.6985	64.6637

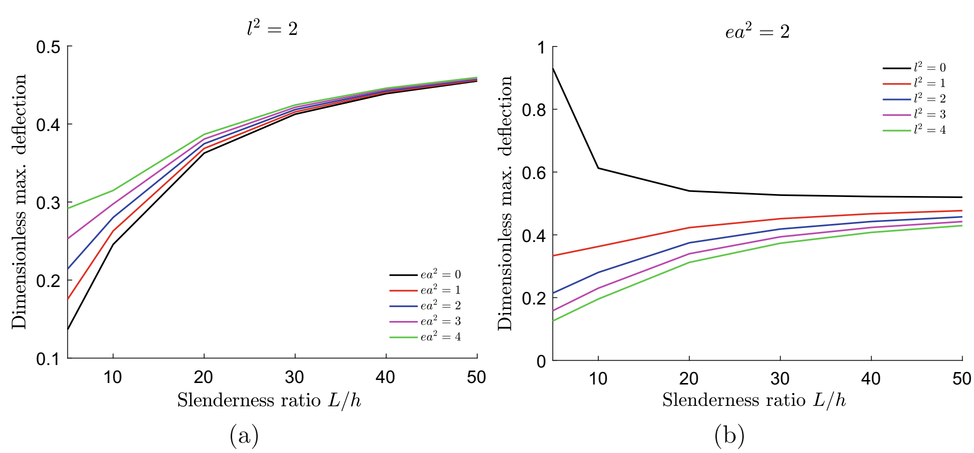

Fig. 5 Clamped-simply supported nanobeam: effect of slenderness ratio (*L*/*h*) on the deflections, **a** for different values of nonlocal parameter with $l^2 = 2$, **b** for different values of strain gradient parameter with $ea^2 = 2$

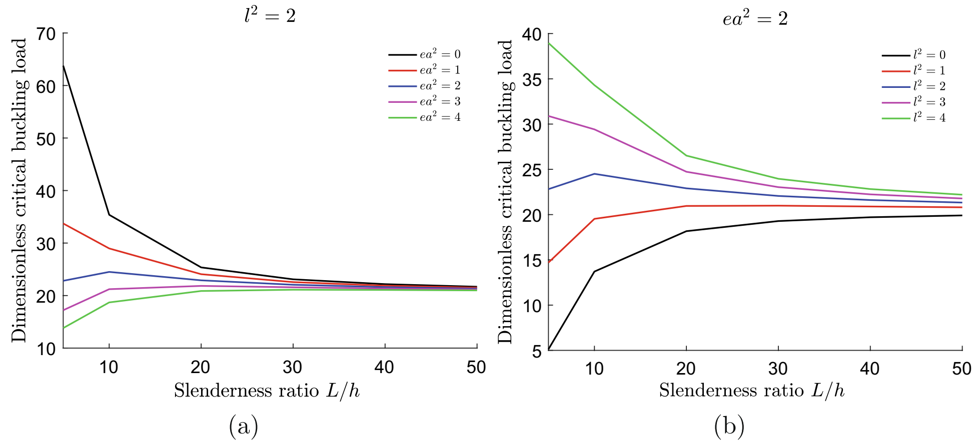

Fig. 6 Clamped-simply supported nanobeam: effect of slenderness ratio (L/h) on the buckling, **a** for different values of nonlocal parameter with $l^2 = 2$, **b** for different values of strain gradient parameter with $ea^2 = 2$

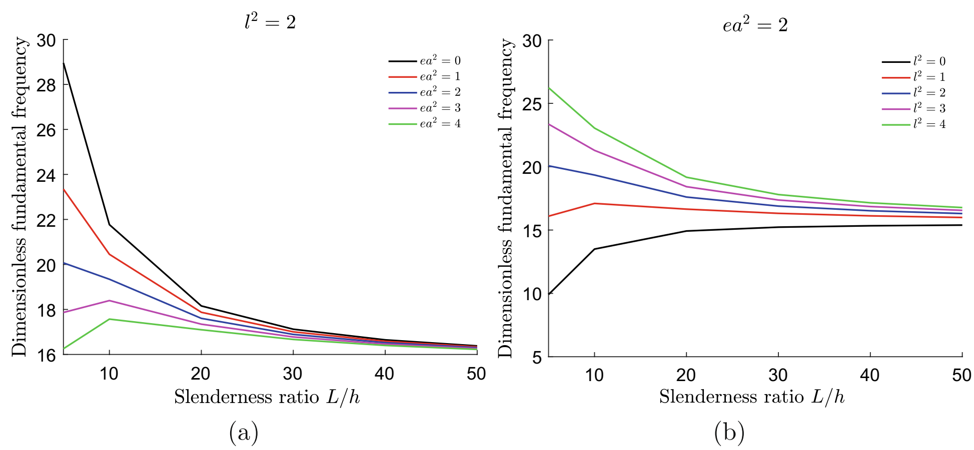

Fig. 7 Clamped-simply supported nanobeam: effect of slenderness ratio (L/h) on the free vibration, **a** for different values of nonlocal parameter with $l^2 = 2$, **b** for different values of strain gradient parameter with $ea^2 = 2$

Table 7 Clamped–clamped nanobeam: dimensionless maximum deflections

ea (nm)	$L/h = 10$			$L/h = 20$			$L/h = 50$		
	$l = 0$ nm	$l = 1$ nm	$l = 2$ nm	$l = 0$ nm	$l = 1$ nm	$l = 2$ nm	$l = 0$ nm	$l = 1$ nm	$l = 2$ nm
0	0.2873	0.1217	0.0521	0.2641	0.1742	0.1076	0.2575	0.2217	0.1854
1	0.2873	0.1217	0.0521	0.2641	0.1742	0.1076	0.2575	0.2217	0.1854
2	0.2873	0.1217	0.0521	0.2641	0.1742	0.1076	0.2575	0.2217	0.1854

Table 8 Clamped–clamped nanobeam: dimensionless buckling loads

L/h	ea (nm)	First buckling load			Second buckling load			Third buckling load		
		$l = 0$ nm	$l = 1$ nm	$l = 2$ nm	$l = 0$ nm	$l = 1$ nm	$l = 2$ nm	$l = 0$ nm	$l = 1$ nm	$l = 2$ nm
5	0	2.4155	3.8287	5.8249	18.1308	39.3600	87.7649	37.9108	136.5981	404.3530
	1	2.1977	3.4132	5.0733	9.5836	18.3065	39.9924	10.9021	52.7773	180.7486
	2	1.7298	2.5469	3.5993	3.4750	11.7276	15.4692	3.9696	15.4980	53.2982
10	0	2.4616	3.0773	3.9339	21.0819	29.9254	46.5778	53.4035	94.7720	195.4781
	1	2.4021	2.9959	3.8182	17.2383	23.9431	36.2702	32.9784	55.5343	112.3988
	2	2.2397	2.7748	3.5059	11.1435	14.7124	21.3196	15.3574	23.9315	49.8174
20	0	2.4734	2.7442	3.0953	21.9796	25.4217	31.3975	59.5513	74.4738	106.6443
	1	2.4582	2.7265	3.0744	20.8192	24.0194	29.5614	51.5669	64.0462	90.7834
	2	2.4136	2.6749	3.0134	17.9724	20.5975	25.1076	36.7749	44.9262	62.2120
50	0	2.4768	2.5709	2.6863	22.2451	23.2645	24.8194	61.5403	65.3204	72.4764
	1	2.4743	2.5683	2.6835	22.0485	23.0556	24.5922	60.0525	63.7166	70.6604
	2	2.4670	2.5606	2.6753	21.4789	22.4507	23.9344	55.9917	59.3429	65.7140

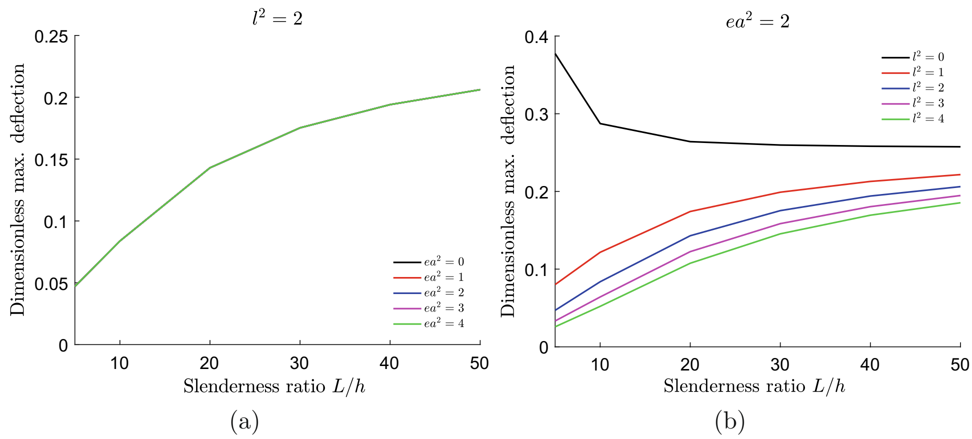

Fig. 8 Clamped–clamped nanobeam: effect of slenderness ratio (*L*/*h*) on the deflections, **a** for different values of nonlocal parameter with $l^2 = 2$, **b** for different values of strain gradient parameter with $ea^2 = 2$

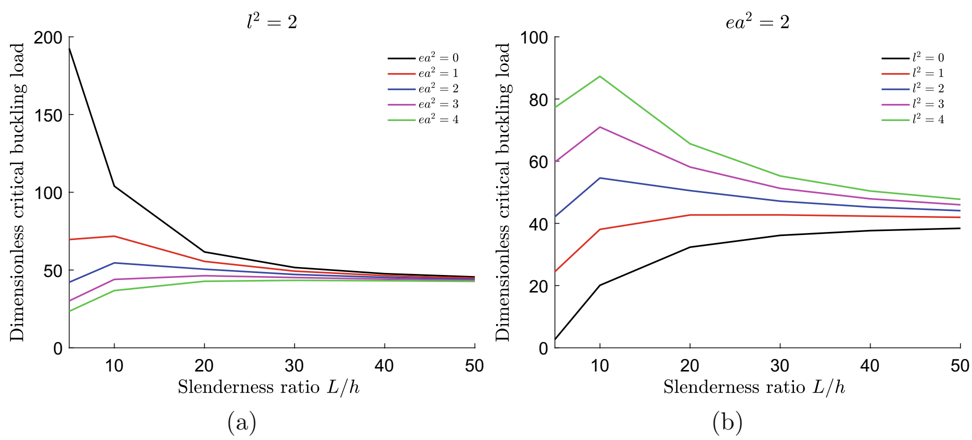

Fig. 9 Clamped–clamped nanobeam: effect of slenderness ratio (*L*/*h*) on the buckling, **a** for different values of nonlocal parameter with $l^2 = 2$, **b** for different values of strain gradient parameter with $ea^2 = 2$

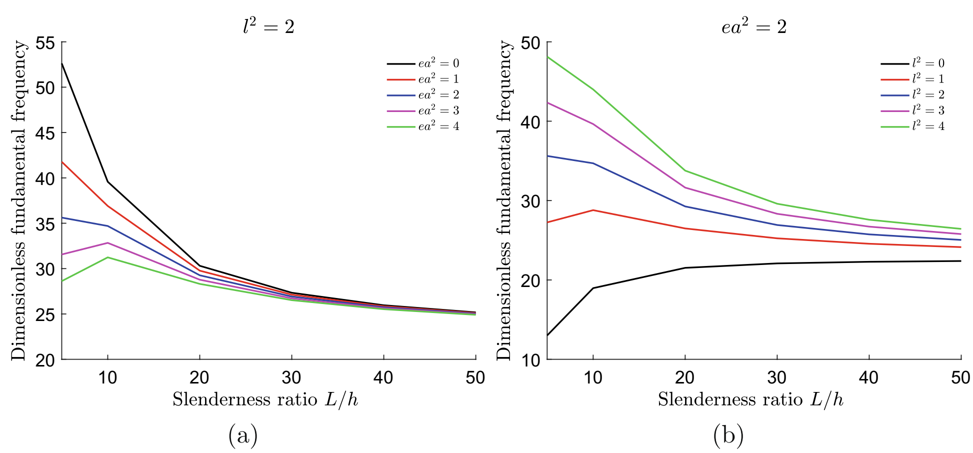

Fig. 10 Clamped–clamped nanobeam: effect of slenderness ratio (*L*/*h*) on the free vibration, **a** for different values of nonlocal parameter with $l^2 = 2$, **b** for different values of strain gradient parameter with $ea^2 = 2$

The last analysis is about cantilevered nano-beams under uniform load and the results are presented in Tables 10, 11 and 12. From these tables, unlike in the case of simply supported or clamped-simply supported beam, the deflection decreases with the increase of the nonlocal parameter *ea* or strain gradient *l*values. However, the decrease in deflection is high compared to those of clamped case. The effect of slenderness ratio on the response of cantilever nanobeams is plotted in Figs. 11, 12 and 13 for different values of nonlocal parameter and strain gradient parameter. The results are qualitatively similar to that of clamped–clamped supported beam.

From the results presented in Tables 4 and 12, we can find an interesting phenomenon is that for clamped–clamped,

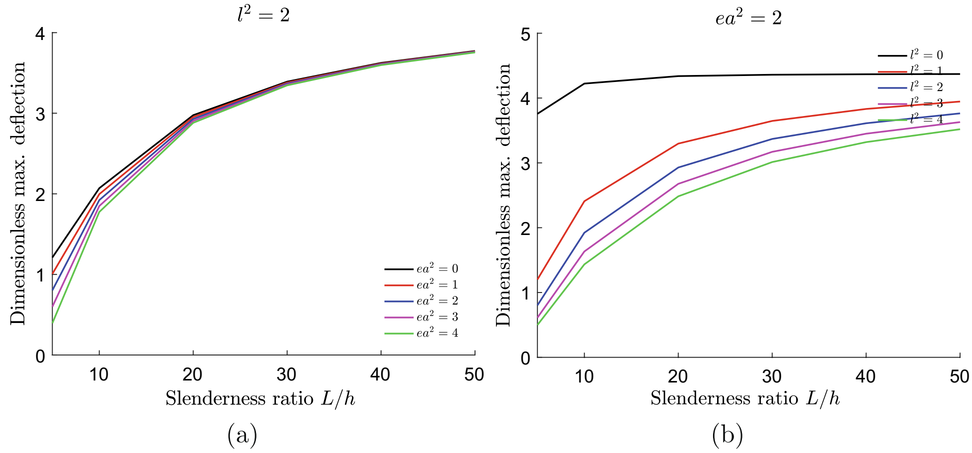

Fig. 11 Cantilever nanobeam: effect of slenderness ratio (*L*/*h*) on the deflections, **a** for different values of nonlocal parameter with $l^2 = 2$, **b** for different values of strain gradient parameter with $ea^2 = 2$

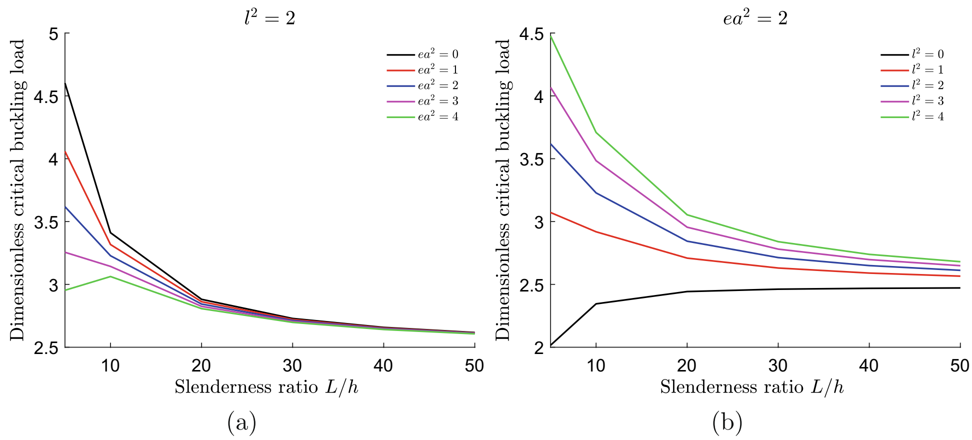

Fig. 12 Cantilever nanobeam: effect of slenderness ratio (*L*/*h*) on the buckling, **a** for different values of nonlocal parameter with $l^2 = 2$, **b** for different values of strain gradient parameter with $ea^2 = 2$

Table 9 Clamped–clamped nanobeam: dimensionless fundamental frequencies

L/*h*	*ea* (nm)	First mode			Second mode			Third mode		
		$l = 0$ nm	$l = 1$ nm	$l = 2$ nm	$l = 0$ nm	$l = 1$ nm	$l = 2$ nm	$l = 0$ nm	$l = 1$ nm	$l = 2$ nm
5	0	3.4254	5.0103	6.7106	18.5342	29.4441	43.0438	27.2417	84.0706	43.0438
	1	3.1515	4.4874	5.8972	12.7079	18.7541	26.9064	23.6772	42.9708	71.6460
	2	2.5946	3.5313	4.5155	8.1506	11.8915	17.2785	13.6783	25.1129	42.3937
10	0	3.5028	4.2674	5.1639	21.0100	26.7584	34.4589	55.3320	76.9570	108.9553
	1	3.4244	4.1545	5.0079	18.3362	22.8261	28.7976	42.2444	56.7013	78.8647
	2	3.2153	3.8596	4.6080	14.0481	17.0436	21.1093	28.6743	37.9554	53.0279
20	0	3.5233	3.8819	4.2973	21.8264	24.4156	27.9957	60.0283	69.4160	84.5772
	1	3.5030	3.8574	4.2678	20.9969	23.4030	26.7284	55.0325	63.1483	76.2705
	2	3.4438	3.7863	4.1825	18.9742	20.9782	23.7531	45.3876	51.4739	61.4571
50	0	3.5292	3.6591	3.8106	22.0758	22.9504	24.0898	61.6279	64.4705	68.8419
	1	3.5259	3.6556	3.8067	21.9337	22.7974	23.9228	60.6962	63.4614	67.7211
	2	3.5161	3.6450	3.7953	21.5227	22.3554	23.4414	58.1370	60.6985	64.6637

Table 10 Cantilever nanobeam: dimensionless maximum deflections

ea (nm)	$L/h = 10$			$L/h = 20$			$L/h = 50$		
	$l = 0$ nm	$l = 1$ nm	$l = 2$ nm	$l = 0$ nm	$l = 1$ nm	$l = 2$ nm	$l = 0$ nm	$l = 1$ nm	$l = 2$ nm
0	4.4712	2.5784	1.5580	4.4005	3.3485	2.5263	4.3805	3.9553	3.5276
1	4.3472	2.4934	1.4961	4.3695	3.3229	2.5050	4.3755	3.9507	3.5233
2	3.9752	2.2386	1.3105	4.2765	3.2460	2.4413	4.3606	3.9369	3.5105

Table 11 Cantilever nanobeam: dimensionless buckling loads

L/h	*ea* (nm)	First buckling load			Second buckling load			Third buckling load		
		$l = 0$ nm	$l = 1$ nm	$l = 2$ nm	$l = 0$ nm	$l = 1$ nm	$l = 2$ nm	$l = 0$ nm	$l = 1$ nm	$l = 2$ nm
5	0	2.4155	3.8287	5.8249	18.1308	39.3600	87.7649	37.9108	136.5981	404.3530
	1	2.1977	3.4132	5.0733	9.5836	18.3065	39.9924	10.9021	52.7773	180.7486
	2	1.7298	2.5469	3.5993	3.4750	11.7276	15.4692	3.9696	15.4980	53.2982
10	0	2.4616	3.0773	3.9339	21.0819	29.9254	46.5778	53.4035	94.7720	195.4781
	1	2.4021	2.9959	3.8182	17.2383	23.9431	36.2702	32.9784	55.5343	112.3988
	2	2.2397	2.7748	3.5059	11.1435	14.7124	21.3196	15.3574	23.9315	49.8174
20	0	2.4734	2.7442	3.0953	21.9796	25.4217	31.3975	59.5513	74.4738	106.6443
	1	2.4582	2.7265	3.0744	20.8192	24.0194	29.5614	51.5669	64.0462	90.7834
	2	2.4136	2.6749	3.0134	17.9724	20.5975	25.1076	36.7749	44.9262	62.2120
50	0	2.4768	2.5709	2.6863	22.2451	23.2645	24.8194	61.5403	65.3204	72.4764
	1	2.4743	2.5683	2.6835	22.0485	23.0556	24.5922	60.0525	63.7166	70.6604
	2	2.4670	2.5606	2.6753	21.4789	22.4507	23.9344	55.9917	59.3429	65.7140

Table 12 Cantilever nanobeam: dimensionless fundamental frequencies

L/h	*ea* (nm)	First mode			Second mode			Third mode		
		$l = 0$ nm	$l = 1$ nm	$l = 2$ nm	$l = 0$ nm	$l = 1$ nm	$l = 2$ nm	$l = 0$ nm	$l = 1$ nm	$l = 2$ nm
5	0	3.4254	5.0103	6.7106	18.5342	29.4441	43.0438	27.2417	84.0706	43.0438
	1	3.1515	4.4874	5.8972	12.7079	18.7541	26.9064	23.6772	42.9708	71.6460
	2	2.5946	3.5313	4.5155	8.1506	11.8915	17.2785	13.6783	25.1129	42.3937
10	0	3.5028	4.2674	5.1639	21.0100	26.7584	34.4589	55.3320	76.9570	108.9553
	1	3.4244	4.1545	5.0079	18.3362	22.8261	28.7976	42.2444	56.7013	78.8647
	2	3.2153	3.8596	4.6080	14.0481	17.0436	21.1093	28.6743	37.9554	53.0279
20	0	3.5233	3.8819	4.2973	21.8264	24.4156	27.9957	60.0283	69.4160	84.5772
	1	3.5030	3.8574	4.2678	20.9969	23.4030	26.7284	55.0325	63.1483	76.2705
	2	3.4438	3.7863	4.1825	18.9742	20.9782	23.7531	45.3876	51.4739	61.4571
50	0	3.5292	3.6591	3.8106	22.0758	22.9504	24.0898	61.6279	64.4705	68.8419
	1	3.5259	3.6556	3.8067	21.9337	22.7974	23.9228	60.6962	63.4614	67.7211
	2	3.5161	3.6450	3.7953	21.5227	22.3554	23.4414	58.1370	60.6985	64.6637

clamped-simply supported and cantilever boundary conditions, when the nonlocal parameter is equal to the material length scale parameter, the buckling loads and natural frequencies predicted by nonlocal strain gradient theory are higher than those obtained by classical continuum theory ($ea = l = 0$), contrary for the case of maximum deflection. This indicates that the combined effects of nonlocal and strain gradient depend not only on the relative magnitude of the two scale parameters but also on the boundary conditions.

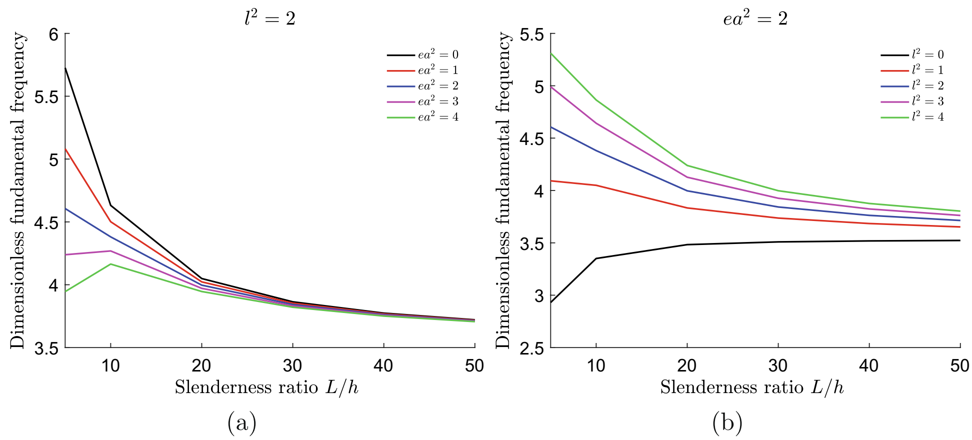

Fig. 13 Cantilever nanobeam: effect of slenderness ratio (L/h) on the free vibration, **a** for different values of nonlocal parameter with $l^2 = 2$, **b** for different values of strain gradient parameter with $ea^2 = 2$

7 Conclusion

The size-dependent bending, vibration and buckling analysis of nanobeams is investigated using finite element approach and based on nonlocal strain gradient theory using a novel two variable trigonometric shear deformation beams theory. The size effects are evaluated by introducing a nonlocal parameter and strain gradient parameter. The robustness and the reliability of the developed finite element model are tested using analytical solutions. Navier's method is employed to get the analytical solutions for bending, vibration and buckling responses of a simply supported nanobeam. A parametric study is conducted to bring out the influence of various parameters such as nonlocal parameter, strain gradient parameter and slenderness ratio considering different boundary conditions. The following main points can be drawn from the present study:

1. The present formulation is in good agreement with those of analytical results and with those of the literature.
2. The response of the nanobeam depends largely on the nonlocal parameter, strain gradient parameter and slenderness ratio and it can be even qualitatively different.
3. With increasing the nonlocal parameter value, the dimensionless deflection value increases, the dimensionless critical buckling load and the frequency value decrease.
4. The nanobeam could exhibit either stiffness-softening effect or stiffness-hardening effect, which depends on the relative magnitude of the nonlocal parameter and the material length scale parameter.

The present novel two-variable theory is not only accurate but also simple in predicting the size-dependent bending, vibration and buckling analysis of nanobeams.

References

1. Lau KT, Gu C, Hui D (2006) A critical review on nanotube and nanotube/nanoclay related polymer composite materials. Compos Part B Eng 37(6):425–436
2. Malekzadeh P, Setoodeh A, Beni AA (2011) Small scale effect on the free vibration of orthotropic arbitrary straight-sided quadrilateral nanoplates. Compos Struct 93(7):1631–1639
3. Bouazza M, Becheri T, Boucheta A, Benseddiq N (2016) Thermal buckling analysis of nanoplates based on nonlocal elasticity theory with four-unknown shear deformation theory resting on Winkler–Pasternak elastic foundation. Int J Comput Methods Eng Sci Mech 17(5–6):362–373
4. Motezaker M, Jamali M, Kolahchi R (2020) Application of differential cubature method for nonlocal vibration, buckling and bending response of annular nanoplates integrated by piezoelectric layers based on surface-higher order nonlocal-piezoelasticity theory. J Comput Appl Math 369:112625
5. Motezaker M, Kolahchi R (2017) Seismic response of concrete columns with nanofiber reinforced polymer layer. Comput Concrete 20(3):361–368
6. Qian Z, Hui Y, Rinaldi M, Liu F, Kar S (2013) Single transistor oscillator based on a graphene-aluminum nitride nano plate resonator. In: 2013 joint European frequency and time forum international frequency control symposium (EFTF/IFC), pp 559–561
7. Tong X, DiLabio GA, Clarkin OJ, Wolkow RA (2004) Ring-opening radical clock reactions for hybrid organic silicon surface nanostructures: a new self-directed growth mechanism and kinetic insights. Nano Lett 4(2):357–360
8. Reddy B, Dorvel BR, Go J et al (2011) High-k dielectric Al2O3 nanowire and nanoplate field effect sensors for improved PH sensing. Biomed Microdev 13(2):335–44
9. Zhang Y, Chang G, Liu S, Lu W, Tian J, Sun X (2011) A new preparation of au nanoplates and their application for glucose sensing. Biosens Bioelectron 28(1):344–348
10. Ding J, Zhang K, Wei G, Su Z (2015) Fabrication of polypyrrole nanoplates decorated with silver and gold nanoparticles for sensor applications. RSC Adv 5:69745–69752
11. Tang X, Lai KWC (2014) Quantitative study of AFM-based nanopatterning of graphene nanoplate. In: 14th IEEE International Conference on Nanotechnology, pp 54–57
12. Jeong W, Lee M, Lee H, Lee H, Kim B, Park JY (2016) Ultraflat au nanoplates as a new building block for molecular electronics. Nanotechnology 27(21):215601

13. Nan T, Hui Y, Rinaldi M, Sun NX (2013) Self-Biased 215MHz Magnetoelectric NEMS Resonator for Ultra-Sensitive DC Magnetic Field Detection. Scientific Reports 3
14. Hui Y, Gomez-Diaz JS, Qian Z, Alù A, Rinaldi M (2016) Plasmonic piezoelectric nanomechanical resonator for spectrally selective infrared sensing. Nat Commun 7:11249
15. Ekinci KL, Roukes ML (2005) Nanoelectromechanical systems. Rev Sci Instrum 76(6):061101
16. Houari MSA, Bessaim A, Bernard F, Tounsi A, Hassan S (2018) Buckling analysis of new quasi-3D FG nanobeams based on nonlocal strain gradient elasticity theory and variable length scale parameter. Steel Compos Struct 28:13–24
17. Lu L, Guo X, Zhao J (2017) Size-dependent vibration analysis of nanobeams based on the nonlocal strain gradient theory. Int J Eng Sci 116:12–24
18. Lu L, Guo X, Zhao J (2017) A unified nonlocal strain gradient model for nanobeams and the importance of higher order terms. Int J Eng Sci 119:265–277
19. Eringen A (1972) Nonlocal polar elastic continua. Int J Eng Sci 10(1):1–16
20. Eringen AC (1983) On differential equations of nonlocal elasticity and solutions of screw dislocation and surface waves. J Appl Phys 54(9):4703–4710
21. Mindlin RD (1964) Micro-structure in linear elasticity. Arch Ration Mech Anal 16:51–78
22. Mindlin R (1965) Second gradient of strain and surface-tension in linear elasticity. Int J Solids Struct 1(4):417–438
23. Papargyri-Beskou S, Tsepoura K, Polyzos D, Beskos D (2003) Bending and stability analysis of gradient elastic beams. Int J Solids Struct 40(2):385–400
24. Yang F, Chong A, Lam D, Tong P (2002) Couple stress based strain gradient theory for elasticity. Int J Solids Struct 39(10):2731–2743
25. Askes H, Aifantis EC (2009) Gradient elasticity and flexural wave dispersion in carbon nanotubes. Phys Rev B 80:195412
26. Civalek Ömer, Demir Çiğdem (2011) Bending analysis of microtubules using nonlocal Euler–Bernoulli beam theory. Appl Math Model 35(5):2053–2067
27. Eltaher M, Khater M, Emam SA (2016) A review on nonlocal elastic models for bending, buckling, vibrations, and wave propagation of nanoscale beams. Appl Math Model 40(5):4109–4128
28. Barati MR, Zenkour AM, Shahverdi H (2016) Thermo-mechanical buckling analysis of embedded nanosize FG plates in thermal environments via an inverse cotangential theory. Compos Struct 141:203–212
29. Merzouki T, Ganapathi M, Polit O (2017) A nonlocal higher-order curved beam finite model including thickness stretching effect for bending analysis of curved nanobeams. Mech Adv Mater Struct 26:1–17
30. Ganapathi M, Merzouki T, Polit O (2018) Vibration study of curved nanobeams based on nonlocal higher-order shear deformation theory using finite element approach. Compos Struct 184:821–838
31. Thai H-T, Vo TP, Nguyen T-K, Kim S-E (2017) A review of continuum mechanics models for size-dependent analysis of beams and plates. Compos Struct 177:196–219
32. Fleck N, Hutchinson J (1993) A phenomenological theory for strain gradient effects in plasticity. J Mech Phys Solids 41(12):1825–1857
33. Lam D, Yang F, Chong A, Wang J, Tong P (2003) Experiments and theory in strain gradient elasticity. J Mech Phys Solids 51(8):1477–1508
34. Stölken J, Evans A (1998) A microbend test method for measuring the plasticity length scale. Acta Mater 46(14):5109–5115
35. Ebrahimi F, Barati MR, Dabbagh A (2016) A nonlocal strain gradient theory for wave propagation analysis in temperature-dependent inhomogeneous nanoplates. Int J Eng Sci 107:169–182
36. Reddy J (2011) Microstructure-dependent couple stress theories of functionally graded beams. J Mech Phys Solids 59(11):2382–2399
37. Li Y, Feng W, Cai Z (2014) Bending and free vibration of functionally graded piezoelectric beam based on modified strain gradient theory. Compos Struct 115:41–50
38. Mohammadimehr M, Farahi MJ, Alimirzaei S (2016) Vibration and wave propagation analysis of twisted micro-beam using strain gradient theory. Appl Math Mech 37(10):1375–1392
39. Li L, Hu Y, Ling L (2015) Flexural wave propagation in small-scaled functionally graded beams via a nonlocal strain gradient theory. Compos Struct 133:1079–1092
40. Li L, Li X, Hu Y (2016) Free vibration analysis of nonlocal strain gradient beams made of functionally graded material. Int J Eng Sci 102:77–92
41. Xu X-J, Wang X-C, Zheng M-L, Ma Z (2017) Bending and buckling of nonlocal strain gradient elastic beams. Compos Struct 160:366–377
42. Li X, Li L, Hu Y, Ding Z, Deng W (2017) Bending, buckling and vibration of axially functionally graded beams based on nonlocal strain gradient theory. Compos Struct 165:250–265
43. Sahmani S, Aghdam MM, Rabczuk T (2018) Nonlinear bending of functionally graded porous micro/nano-beams reinforced with graphene platelets based upon nonlocal strain gradient theory. Compos Struct 186:68–78
44. Allam MNM, Radwan AF (2019) Nonlocal strain gradient theory for bending, buckling, and vibration of viscoelastic functionally graded curved nanobeam embedded in an elastic medium. Adv Mech Eng 11(4):1687814019837067
45. Radwan AF, Sobhy M (2018) A nonlocal strain gradient model for dynamic deformation of orthotropic viscoelastic graphene sheets under time harmonic thermal load. Physica B 538:74–84
46. Ghugal YM, Shimpi RP (2001) A review of refined shear deformation theories for isotropic and anisotropic laminated beams. J Reinf Plast Compos 20(3):255–272
47. Motezaker M, Eyvazian A (2020) Buckling load optimization of beam reinforced by nanoparticles. Struct Eng Mech 73(5):481–486
48. Castellazzi G, Krysl P, Bartoli I (2013) A displacement-based finite element formulation for the analysis of laminated composite plates. Compos Struct 95:518–527
49. Reddy JN (1984) A simple higher-order theory for laminated composite plates. ASME J Appl Mech 51(4):745–752
50. Kolahchi R, Hosseini H, Fakhar MH, Taherifar R, Mahmoudi M (2019) A numerical method for magneto-hygro-thermal postbuckling analysis of defective quadrilateral graphene sheets using higher order nonlocal strain gradient theory with different movable boundary conditions. Comput Math Appl 78(6):2018–2034
51. Daikh AA, Bensaid I, Zenmour AM (2020) Temperature dependent thermomechanical bending response of functionally graded sandwich plates. Eng Res Express 2(1):015006
52. Touratier M (1991) An efficient standard plate theory. Int J Eng Sci 29(8):901–916
53. Soldatos K (1992) A transverse shear deformation theory for homogeneous monoclinic plates. Acta Mech 94(3–4):195–220
54. Keshtegar B, Bagheri M, Meng D, Kolahchi R, Trung N-T (2020) Fuzzy reliability analysis of nanocomposite zno beams using hybrid analytical-intelligent method. Eng Comput 1–16
55. Keshtegar B, Tabatabaei J, Kolahchi R, Trung N-T (2020) Dynamic stress response in the nanocomposite concrete pipes with internal fluid under the ground motion load. Adv Concrete Construct 9(3):327–335
56. Karama M, Afaq K, Mistou S (2003) Mechanical behaviour of laminated composite beam by the new multi-layered laminated

composite structures model with transverse shear stress continuity. Int J Solids Struct 40(6):1525–1546
57. Hajmohammad MH, Kolahchi R, Zarei MS, Nouri AH (2019) Dynamic response of auxetic honeycomb plates integrated with agglomerated CNT-reinforced face sheets subjected to blast load based on visco-sinusoidal theory. Int J Mech Sci 153:391–401
58. Farokhian A, Kolahchi R (2020) Frequency and instability responses in nanocomposite plate assuming different distribution of CNTS. Struct Eng Mech 73(5):555–563
59. Thai H-T (2012) A nonlocal beam theory for bending, buckling, and vibration of nanobeams. Int J Eng Sci 52:56–64
60. Levy M (1877) Mémoire sur la théorie des plaques élastiques planes. Journal de mathématiques pures et appliquées 219–306
61. Abualnour M, Houari MSA, Tounsi A, Mahmoud S et al (2018) A novel quasi-3D trigonometric plate theory for free vibration analysis of advanced composite plates. Compos Struct 184:688–697
62. Eringen AC (1972) Nonlocal polar elastic continua. Int J Eng Sci 10:1–16
63. Eringen AC, Edelen DGB (1972) On nonlocal elasticity. Int J Eng Sci 10:233–248
64. Eringen AC (1983) On differential equations of nonlocal elasticity and solutions of screw dislocation and surface waves. J Appl Phys 54:4703–4710
65. Aifantis K, Willis J (2005) The role of interfaces in enhancing the yield strength of composites and polycrystals. J Mech Phys Solids 53(5):1047–1070
66. Aifantis EC (1992) On the role of gradients in the localization of deformation and fracture. Int J Eng Sci 30(10):1279–1299
67. Lim C, Zhang G, Reddy J (2015) A higher-order nonlocal elasticity and strain gradient theory and its applications in wave propagation. J Mech Phys Solids 78:298–313
68. Li L, Hu Y, Ling L (2016) Wave propagation in viscoelastic single-walled carbon nanotubes with surface effect under magnetic field based on nonlocal strain gradient theory. Physica E 75:118–124
69. Mouffoki A, Adda Bedia E, Mohammed Sid Ahmed H, Tounsi A, Hassan S (2017) Vibration analysis of nonlocal advanced nanobeams in hygro-thermal environment using a new two-unknown trigonometric shear deformation beam theory. Smart Struct Syst 20:369–383
70. Li L, Hu Y, Li X (2016) Longitudinal vibration of size-dependent rods via nonlocal strain gradient theory. Int J Mech Sci 115–116:135–144

Publisher's Note Springer Nature remains neutral with regard to jurisdictional claims in published maps and institutional affiliations.